Molecular Basis for Interactions of G Protein βγ Subunits with Effectors

Carolyn E. Ford,* Nikolai P. Skiba,* Hyunsu Bae, Yehia Daaka, Eitan Reuveny, Lee R. Shekter, Ramon Rosal, Gezhi Weng, Chii-Shen Yang, Ravi Iyengar, Richard J. Miller, Lily Y. Jan, Robert J. Lefkowitz, Heidi E. Hamm†

Both the α and βγ subunits of heterotrimeric guanine nucleotide–binding proteins (G proteins) communicate signals from receptors to effectors. Gβγ subunits can regulate a diverse array of effectors, including ion channels and enzymes. Gα subunits bound to guanine diphosphate (Gα-GDP) inhibit signal transduction through Gβγ subunits, suggesting a common interface on Gβγ subunits for Gα binding and effector interaction. The molecular basis for interaction of Gβγ with effectors was characterized by mutational analysis of Gβ residues that make contact with Gα-GDP. Analysis of the ability of these mutants to regulate the activity of calcium and potassium channels, adenylyl cyclase 2, phospholipase C-β2, and β-adrenergic receptor kinase revealed the Gβ residues required for activation of each effector and provides evidence for partially overlapping domains on Gβ for regulation of these effectors. This organization of interaction regions on Gβ for different effectors and Gα explains why subunit dissociation is crucial for signal transmission through Gβγ subunits.

Upon receptor activation, G proteins dissociate into free Gα and Gβγ subunits that can activate various effectors (*1*). Effector proteins of the Gβγ complex include phospholipases (*2*), adenylyl cyclases (*3*), ion channels (*4*), G protein–coupled receptor kinases (*5*) and phosphoinositide 3-kinases (*6*). Other potential Gβγ effectors include dynamin I and the nonreceptor protein tyrosine kinases Btk and Tsk (*7*). GDP-bound Gα subunits (Gα-GDP) can compete with Gβγ effectors and deactivate Gβγ-dependent signaling, suggesting that Gβγ may use a common binding surface for interaction with Gα and with its diverse effectors. Two regions on Gβγ that interact with Gα have been defined by the crystal structures of heterotrimeric Gαβγ (*8*), the switch interface (Gβ residues 57, 59, 98, 99, 101, 117, 119, 143, 186, 228, and 332) and the NH_2-terminal interface (Gβ residues 55, 78, 80 and 89). Each of these residues on retinal Gβ (Gβ1) was substituted with alanine, and each Gβ1 mutant was expressed with either Gγ1 or Gγ2, two isoforms of the Gγ subunit. All mutated Gβ1γ1 dimers were folded properly, were post-translationally modified appropriately, and were expressed at similar amounts as in the wild type (*9*). The Gβγ mutants were tested for their ability to assemble into heterotrimers with Gα, to be activated by rhodopsin, and to interact with Gβγ downstream signaling partners: β-adrenergic receptor kinase (βARK), phospholipase C-β2 (PLC-β2), adenylyl cyclase 2 (AC2), muscarinic potassium channel (GIRK1/GIRK4), and the calcium channel α1B subunit (CCα1B).

To determine whether purified $Gβ1H_6γ1$ mutants could form heterotrimers, we measured the ability of the Gβγ mutants to facilitate pertussis toxin–catalyzed adenosine diphosphate (ADP) ribosylation of transducin Gα-GDP (Gtα) (*10*). All mutants could support some level of ADP ribosylation, although Gβ mutants $Ile^{80} \rightarrow Ala^{80}$ (I80A), K89A, L117A, and W332A (*11*) showed reduced ability to form heterotrimers (Fig. 1A).

Because Gβγ is essential for functional heterotrimer interaction with activated receptors that catalyze the exchange of GDP for guanosine triphosphate (GTP) on the Gα subunit, we also measured the ability of the Gβ mutants to support light-activated rhodopsin-catalyzed nucleotide exchange on the α subunit of transducin (Gtα) (*12*). All switch interface mutants (except K57A and Y59A) and the NH_2-terminal interface mutants I80A and K89A were defective in formation of functional heterotrimers (Fig. 1B). Some Gβ mutants were impaired in both assays, indicating that residues 80, 89, 117, and 332 of Gβ are the major determinants of binding to Gtα. The switch interface mutants (S98A, W99A, M101A, N143A, and D186A) were normal in heterotrimer assembly, but were impaired functionally in supporting receptor-catalyzed nucleotide ex-

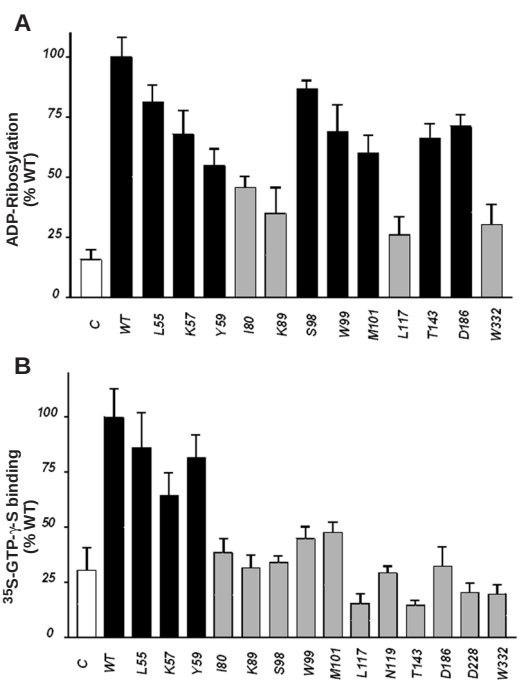

Fig. 1. Effects of $Gβ1H_6γ1$ on heterotrimer assembly and receptor interaction. The data are the normalized percentage of wild-type (WT) recombinant Gβγ activity. (**A**) The ability of recombinant $Gβ1H_6γ1$ and Gβ1 mutants to assemble into heterotrimers with Gtα was determined by testing whether pertussis toxin could ADP-ribosylate Gtα with [^{32}P]nicotinamide adenine dinucleotide (*10*). The Gβ residue mutated to alanine is indicated by a number beneath each bar in the figure. Clear bar (C) represents the basal amount of ADP-ribosylation of Gtα that occurred in absence of Gβγ. (**B**) The ability of recombinant $Gβ1H_6γ1$ and Gβ1 mutants to bind Gtα and interact with rhodopsin was determined by the amount of [^{35}S]GTP-γ-S binding catalyzed by light-activated rhodopsin (*12*). Clear bar (C) is the basal amount of [^{35}S]GTP-γ-S binding to Gtα in the presence of urea-washed rod outer segment membranes (50 nM) without added Gβγ. The data represent the mean ± SEM of duplicate determinations in three independent experiments. Alanine mutants that have a distinguishable activity from the wild type are indicated by gray bars; those with activity similar to the wild type are indicated by black bars (*11*).

C. E. Ford, N. P. Skiba, H. Bae, C.-S. Yang, H. E. Hamm, Institute for Neuroscience and Department of Molecular Pharmacology and Biological Chemistry, Northwestern University, Chicago, IL 60611, USA.
Y. Daaka and R. J. Lefkowitz, Howard Hughes Medical Institute and Department of Medicine, Duke University Medical Center, Durham, NC 27710, USA.
E. Reuveny, Department of Membrane Research and Biophysics, Weizmann Institute of Science, Rehovot 76100, Israel.
L. R. Shekter and R. J. Miller, Department of Pharmacological and Physiological Sciences, University of Chicago, Chicago, IL 60637, USA.
R. Rosal, G. Weng, R. Iyengar, Department of Pharmacology, Mount Sinai School of Medicine, New York, NY 10029, USA.
L. Y. Jan, Howard Hughes Medical Institute and Department of Physiology and Biochemistry, University of California at San Francisco, San Francisco, CA 94143, USA.

*These authors contributed equally to this work.
†To whom correspondence should be addressed. E-mail: h-hamm@nwu.edu

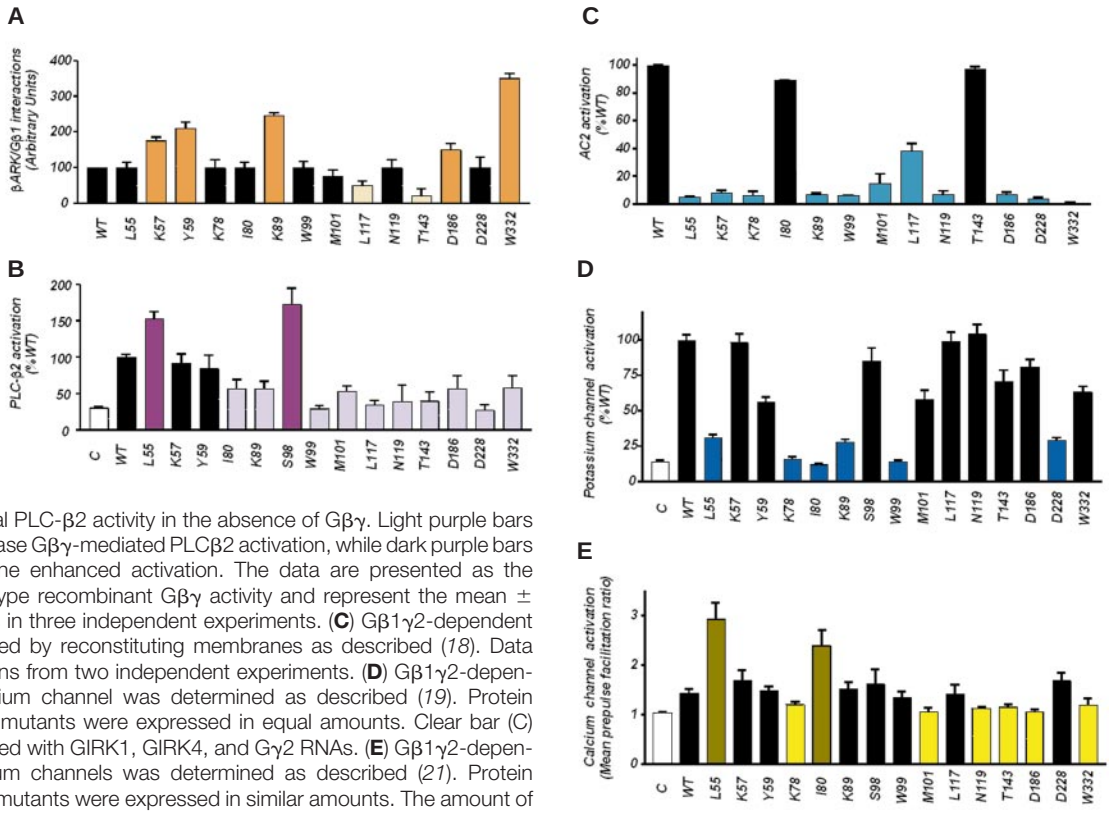

Fig. 2. Gβγ-dependent interactions with βARK, PLC-β2, AC2, muscarinic potassium channel, and CCα1B-containing calcium channel. (**A**) The amount of Gβ1 present in βARK immune complexes was detected as described (*14*). Light orange bars show those mutations that decrease Gβγ/βARK interaction, while dark orange bars show mutations that increase the interaction. The data contained in the bar graph represent duplicate determinations in two independent experiments. (**B**) Gβ1γ1-dependent activation of PLC-β2 was determined as described (*17*). Clear bar (C) represents the basal PLC-β2 activity in the absence of Gβγ. Light purple bars show those mutations that decrease Gβγ-mediated PLCβ2 activation, while dark purple bars indicate mutations that determine enhanced activation. The data are presented as the normalized percentage of wild-type recombinant Gβγ activity and represent the mean ± SEM of duplicate determinations in three independent experiments. (**C**) Gβ1γ2-dependent activation of AC2 was determined by reconstituting membranes as described (*18*). Data represent duplicate determinations from two independent experiments. (**D**) Gβ1γ2-dependent activation of GIRK potassium channel was determined as described (*19*). Protein immunoblotting showed that all mutants were expressed in equal amounts. Clear bar (C) represents control oocytes injected with GIRK1, GIRK4, and Gγ2 RNAs. (**E**) Gβ1γ2-dependent inhibition of CCα1B calcium channels was determined as described (*21*). Protein immunoblotting revealed that all mutants were expressed in similar amounts. The amount of Gβγ-dependent inhibition was calculated as a ratio of the mean prepulse facilitation (MPF) in either the absence or presence of Gβγ. MPF is the statistically averaged relief of the channel inhibition by use of a large depolarizing prepulse. Clear bar (C) represents channel activity in absence of Gβγ. The light yellow bars indicate the Gβ1 mutations that decrease channel modulation and lead to calcium currents that are statistically indistinguishable from the basal calcium current ($P < 0.1$ for K78A and W332A mutants and $P < 0.01$ for M101A, N119A, T143A, and D186A mutants). The dark yellow bars indicate Gβ1 mutants that have increased inhibitory activity ($P < 0.001$ for L55A mutant and $P < 0.01$ for I80A mutant).

change on Gtα. This observation indicates that Gβγ may actively participate in receptor-catalyzed nucleotide exchange, rather than being simply a passive binding partner in receptor–G protein interactions.

Gβγ mediates translocation of G protein–coupled receptor kinases from the cytosol to the membrane, in order that these kinases can phosphorylate activated G protein–coupled receptors and initiate receptor internalization (*13*). The Gβ mutants varied in their ability to associate with βARK1 (Fig. 2A) (*14*). Alanine mutations at Gβ residues 117 and 143 resulted in decreased binding to βARK1. In contrast, alanine mutations at Gβ residues 57, 59, 89, 186, and 332 of Gβ led to increased binding to βARK1. The mutations that resulted in decreased binding are found on the left side of the Gβ surface (Fig. 3) and likely form the βARK binding interface, whereas those mutations that led to increased binding were clustered together at the middle of the structure (Gβ residues 57, 59, and 332) or are at the right side of the surface (Gβ residue 89).

Gβγ is an important modulator of various isoforms of phospholipase C–β (*2*, *15*) and adenylyl cyclase (*16*), effectors that regulate intracellular concentration of second messengers inositol 1,4,5-triphosphate and cyclic adenosine 3′,5′-monophosphate. The ability of the Gβγ mutants to stimulate the activity of PLC-β2 was determined by quantitating the amount of inositol 1,4,5-triphosphate produced by the purified enzyme in the presence of the Gβγ mutants (*17*). Some 13 of the 15 Gα-interacting residues of Gβ we tested were important for Gβγ-dependent activation of PLC-β2, suggesting that Gα and PLC-β binding regions on Gβ are overlapping (Fig. 2B). Mutants W99A and D228A no longer activated PLC-β2 and mutants I80A, K89A, M101A, L117A, N119A, T143A, D186A, and W332A were less effective than wild-type Gβγ. Mutants L55A and S98A activated PLC-β2 to a greater extent than wild-type Gβγ. These residues are circled in magenta on the Gβγ surface (Fig. 3). The effects of the Gβγ mutants on AC2 activation were determined in vitro (*18*) in the presence of constitutively activated Gsα that has glutamine at residue 227 mutated to leucine (Q227L). All the Ala mutations of Gβ residues, except I80A and T143A, had decreased ability to activate AC2 (Fig. 2C); their locations on the Gβγ structure are indicated in teal (Fig. 3).

We also measured K^+ currents in *Xenopus laevis* oocytes injected with RNAs for GIRK1/GIRK4 and Gβγ mutants (*19*). The ability of Gβγ to increase conductance through the muscarinic potassium channel GIRK1/GIRK4 was disrupted by alanine mutations at Gβ residues 55, 78, 80, 89, 99, and 228 (Fig. 2D). All these Gβ residues except W99 and D228 cluster within the NH_2-terminal interface of Gβ (Fig. 3; blue lines).

Gβγ inhibits the activity of certain calcium channels (*20*). We measured the ability of Gβγ mutants to inhibit the conductance of Ca^{2+} channels in HEK 293 cells expressing CCα1B-containing Ca^{2+} channels and Gβγ mutants (*21*). Alanine mutations of Gβ residues 55 and 80, which lie close together at the top of Gβ, had enhanced ability to inhibit current through CCα1B-containing Ca^{2+} channels (Fig. 2E). Alanine mutations of Gβ residues 78, 101, 119, 143, 186, and 332 were no longer able to inhibit current through calcium channels.

Our results demonstrate that many of the Gα-interacting residues of Gβ are important in interactions between Gβγ and

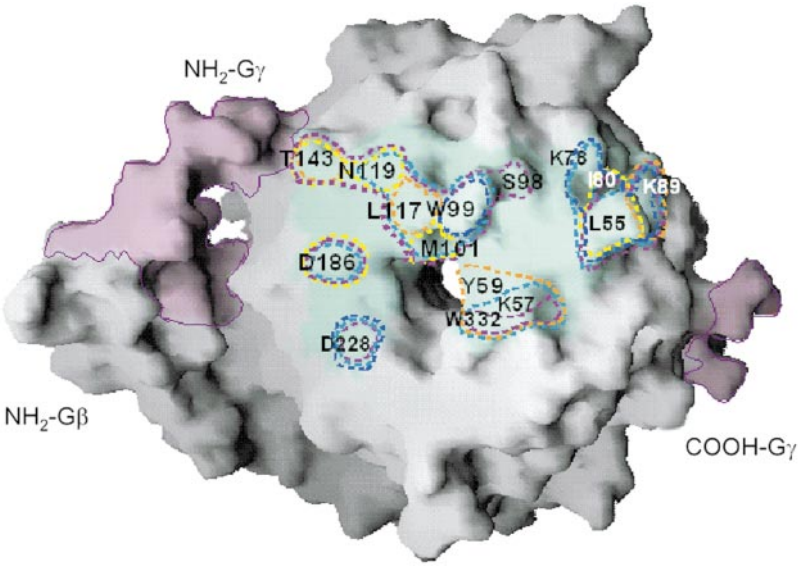

Fig. 3. A schematic representation of the regions of Gβ involved in interactions with effectors and Gα subunit. The crystal coordinates of Gβ1γ1 [Protein Databank entry 1tbg; (*8, 26*)] were used to generate a surface model of the dimer in GRASP. Gβ is gray, and Gγ is pink. The pale green surface is the area on Gβγ that is covered by Gα in the G protein heterotrimer crystal structure. The effector-interacting residues on Gβ are circled with a different color for each effector: orange, βARK; magenta, PLC-β2; teal, AC2; blue, potassium channel; and yellow, calcium channel. Gα-GDP, when bound to Gβγ, covers all these distinct yet partially overlapping effector interaction regions on Gβ and, thus, blocks Gβγ regulation of all the effectors. This figure and other more detailed figures showing residues interacting with individual effectors can be viewed at www.sciencemag.org/feature/data/976104.shl

its signaling partners, and show the functional importance of individual amino acids in the signal transfer from Gβγ to effector activation. Alanine mutation of these Gβ residues may increase, decrease, or abolish Gβγ-dependent interactions. It was unexpected to find Gβγ mutants that are better than the wild type at stimulating the activity of PLC-β2 and inhibiting Ca^{2+} channels. One possible reason for such "gain-of-function" mutations is that turn-off of Gβγ-mediated signaling requires Gα-GDP competition with effectors. The normal side chains at these positions may be destabilizing to effector interaction resulting in a lower affinity in order to allow reassembly of heterotrimeric Gαβγ.

Each signaling partner for Gβ relies on a different subset of Gβ residues for its interaction and hence, creates a set of unique "footprints" on Gβ (Fig. 3). These results are consistent with studies that have suggested a common effector binding surface on Gβγ located near the region of residues 70 to 145 of Gβ (*22*). These data raise an interesting issue of how G proteins and their effectors are oriented with respect to the membrane and whether their orientations change during subunit dissociation and activation (*8, 23*). The Gα-binding surface on Gβγ may not be the only region of effector interaction. Other Gβγ regions of effector interactions that have been implicated are the coiled-coil interface at the NH_2-termini of Gβ and Gγ (*24*) and the COOH-terminal region of Gβ (*25*).

The alanine mutations of Gα-interacting Gβ residues provide an initial framework to determine how Gβγ subunits interact with and regulate so many different effectors that have so little structural similarity. Our studies show that the effector interaction regions are clustered on Gβ such that they partially overlap one another (Fig. 3). This mode of clustering allows for one key regulator (Gα) to regulate Gβγ signal transmission to multiple effectors.

REFERENCES AND NOTES

1. H. E. Hamm, *J. Biol. Chem.* **273**, 669 (1998); E. J. Neer, *Cell* **80**, 249 (1995); D. E. Clapham and E. J. Neer, *Annu. Rev. Pharmacol. Toxicol.* **37**, 167 (1997).
2. S. G. Rhee and Y. S. Bae, *J. Biol. Chem.* **272**, 15045 (1997).
3. R. K. Sunahara, C. W. Dessauer, A. G. Gilman, *Annu. Rev. Pharmacol. Toxicol.* **36**, 461 (1996).
4. T. Schneider, P. Igelmund, T. Hescheler, *Trends Pharmacol. Sci.* **18**, 8 (1997).
5. J. A. Pitcher *et al.*, *Science* **257**, 1264 (1992); N. J. Freedman and R. J. Lefkowitz, *Recent Prog. Horm. Res.* **51**, 319 (1996).
6. B. Vanhaesebroeck, S. J. Leevers, G. Panayotou, M. D. Waterfield, *Trends Biochem. Sci.* **22**, 267 (1997).
7. H. C. Lin and A. G. Gilman, *J. Biol. Chem.* **271**, 27979 (1996); S. A. Langhans-Rajasekaran, Y. Wan, X. Y. Huang, *Proc. Natl. Acad. Sci. U.S.A.* **92**, 8601 (1995).
8. D. G. Lambright *et al.*, *Nature* **379**, 311 (1996); M. A. Wall *et al.*, *Cell* **83**, 1047 (1995).
9. Cloning of hexahistidine-tagged Gγ1 (H_6Gγ1), generation of the Gβ1 and H_6Gγ1 recombinant baculoviruses, detailed protocols for recombinant protein expression in Sf9 insect cells, and detailed protocols for purification of Gβγ complexes are described at www.sciencemag.org/feature/data/976104.shl#9. The recombinant wild-type Gβγ was equivalent to native Gβγ in the assays used in our study. All mutated Gβ1 subunits assembled properly with H_6Gγ1 subunits as judged by the trypsin protection assay. We determined, with mass spectrometry, that the recombinant Gβγ dimers tested were properly modified by isoprenylation and carboxymethylation.
10. The pertussis toxin–catalyzed ADP ribosylation assay was done essentially as described [T. Katada *et al.*, *Methods Enzymol.* **237**, 131 (1994)]. Details of modifications are provided at www.sciencemag.org/feature/data/976104.shl#10.
11. Single-letter abbreviations for the amino acid residues are as follows: A, Ala; C, Cys; D, Asp; E, Glu; F, Phe; G, Gly; H, His; I, Ile; K, Lys; L, Leu; M, Met; N, Asn; P, Pro; Q, Gln; R, Arg; S, Ser; T, Thr; V, Val; W, Trp; and Y, Tyr.
12. Rhodopsin-catalyzed [^{35}S]GTP-γ-S binding assay was done essentially as described [N. P. Skiba *et al.*, *J. Biol. Chem.* **271**, 413 (1996)]. Details of modifications are described at www.sciencemag.org/feature/data/976104.shl#12.
13. R. H. Stoffel, J. A. Pitcher, R. J. Lefkowitz, *J. Membr. Biol.* **157**, 1 (1997).
14. COS-7 cells were transiently transfected with either Gβ1 or Gβ1 mutant, Gγ2, and βARK1 cDNAs (2 μg). The amount of Gβ1 associated with βARK was determined as described [Y. Daaka *et al.*, *Proc. Natl. Acad. Sci. U.S.A.* **94**, 2180 (1997).
15. M. Camps *et al.*, *Nature* **360**, 684 (1992); A. Katz, D. Wu, M. I. Simon, *ibid.*, p. 686.
16. W.-J. Tang and A. G. Gilman, *Science* **254**, 1500 (1991).
17. M. De Vivo, *Methods Enzymol.* **238**, 131 (1994); V. Romoser, R. V. Ball, A. Smrcka, *J. Biol. Chem.* **271**, 25071 (1996). Gβ1γ1-dependent activation of PLC-β2 was determined by reconstitution of purified H_6PLC-β2, Gβγ or mutants, and radiolabeled phosphatidylinositol 4,5-diphosphate in a mixed detergent-phospholipid micelle. See www.sciencemag.org/feature/data/976104.shl#17 for details of PLC-β2 expression, purification, and activation assay.
18. J. Chen *et al.*, *Science* **268**, 1166 (1995). In the presence of 0.14% CHAPS detergent, insect cell membranes that expressed recombinant AC2 were mixed with purified constitutively active Q227L-Gsα and insect cells membranes expressing both recombinant H_6Gγ2 and either recombinant wild-type or mutant Gβ1. Details of the assay are described at www.sciencemag.org/feature/data/976104.shl#18.
19. E. Reuveny *et al.*, *Nature* **370**, 143 (1994); C.-L. Huang, P. A. Slesinger, P. J. Casey, Y. N. Jan, L. Y. Jan, *Neuron* **15**, 1133 (1995). RNAs for either Gβ1 or Gβ1 mutants, Gγ2, GIRK1, and GIRK4 were injected into *Xenopus* oocytes, and the K^+ current was measured by voltage clamp after 3 to 5 days. For details, see www.sciencemag.org/feature/data/976104.shl#19.
20. S. R. Ikeda, *Nature* **380**, 255 (1996); S. Herlitze *et al.*, *ibid.*, p. 258.
21. L. R. Shekter, R. Taussig, S. E. Gillard, R. J. Miller, *Mol. Pharmacol.* **52**, 282 (1997). The Ca^{2+}-current was measured by the whole-cell patch clamp technique in HEK-293 cells stably expressing the calcium channel CCα1B subunit and ancilliary calcium channel subunits (β1 and α2Bδ) and transiently expressing cDNAs encoding Gβ1 (or mutants) and Gγ2. Refer to www.sciencemag.org/feature/data/976104.shl#21 for details.
22. G. Weng *et al.*, *J. Biol. Chem.* **271**, 26445 (1996); Y. Chen *et al.*, *Proc. Natl. Acad. Sci. U.S.A.* **94**, 2711 (1997); K. Yan and N. Gautam, *J. Biol. Chem.* **271**, 17597 (1996); *ibid.*, **272**, 2056 (1997).
23. J. J. G. Tesmer, R. K. Sunahara, A. G. Gilman, S. R. Sprang, *Science* **278**, 1907 (1997).
24. E. Leberer, D. Dignard, L. Hougan, D. Y. Thomas, M. Whiteway, *EMBO J.* **11**, 4805 (1992); A. V. Grishin, J. L. Weiner, K. J. Blumer, *Mol. Cell. Biol.* **14**, 4571 (1994); S. Pellegrino, S. Zhang, A. Garritsen, W. F. Simonds, *J. Biol. Chem.* **272**, 25360 (1997).
25. S. Zhang, O. A. Coso, R. Collins, J. S. Gutkind, W. F.

Simonds, *J. Biol. Chem.* **271**, 20208 (1996); K. Blüml *et al.*, *EMBO J.* **16**, 4908 (1997); J. Yamauchi, Y. Kaziro, H. Itoh, *J. Biol. Chem.* **272**, 7602 (1997).
26. J. Sondek, A. Bohm, D. G. Lambright, H. E. Hamm, P. B. Sigler, *Nature* **379**, 369 (1996).
27. Recombinant baculovirus containing bovine H_6Gγ2 cDNA was provided by A. Gilman (University of Texas Southwestern Medical Center, Dallas, TX). The H_6-Q227L-Gsα was from T. Patel (University of Tennessee, Memphis). The baculovirus vector encoding human PLC-β2 modified with an NH_2-terminal H_6 tag was provided by A. Smrcka (University of Rochester, NY). We thank K. Schey (Medical University of South Carolina, Charleston) for performing the mass spectrometry analysis on the recombinant Gβγ proteins.
28. Supported as follows: Ford Foundation Fellowship (C.E.F.), American Heart Association Grant-In-Aid (N.P.S.), Aaron Diamond Fellowship (G.W.), and both the Mella and Leon Benziyo Center for Neuroscience and Behavioral Research and the Joseph Cohn Center for Biomembrane Research (E.R.). USPHS grants DA02575, DA02121, MH40165, NS33502, DK42086, and DK44840 (R.J.M.); DK38761 and GM54508 (R.I.); and EY06062 and EY10291 (H.E.H.); Howard Hughes Medical Institute (L.Y.J. and R.J.L.), a National Institutes of Mental Health grant to the Silvio Conte Center for Neuroscience at UCSF (L.Y.J.), and both a Distinguished Investigator Award from the National Association for Research in Schizophrenia and Depression and an American Heart Association Grant-in-Aid (H.E.H.).

26 February 1998; accepted 25 March 1998

Distinct WNT Pathways Regulating AER Formation and Dorsoventral Polarity in the Chick Limb Bud

Mineko Kengaku,*† Javier Capdevila,* Concepción Rodriguez-Esteban,* Jennifer De La Peña, Randy L. Johnson, Juan Carlos Izpisúa Belmonte,‡§ Clifford J. Tabin§

The apical ectodermal ridge (AER) is an essential structure for vertebrate limb development. *Wnt3a* is expressed during the induction of the chick AER, and misexpression of *Wnt3a* induces ectopic expression of AER-specific genes in the limb ectoderm. The genes β-*catenin* and *Lef1* can mimic the effect of *Wnt3a*, and blocking the intrinsic *Lef1* activity disrupts AER formation. Hence, *Wnt3a* functions in AER formation through the β-catenin/LEF1 pathway. In contrast, neither β-*catenin* nor *Lef1* affects the *Wnt7a*-regulated dorsoventral polarity of the limb. Thus, two related *Wnt* genes elicit distinct responses in the same tissues by using different intracellular pathways.

The *Wnt* gene family encodes a group of signaling molecules that are implicated in numerous aspects of morphogenesis in both vertebrates and invertebrates. Several chick *Wnt* genes are expressed in a specialized epithelial structure running along the distal margin of the limb bud, called the apical ectodermal ridge (AER), which is essential for limb morphogenesis (*1*, *2*). *Wnt3a* is the first of these genes to be expressed in the limb. We therefore examined the spatiotemporal pattern of expression of *Wnt3a* in developing limb buds with respect to that of *Fgf8*, the earliest known AER marker during chick development (*3*, *4*) (Fig. 1, A through D) (*5*).

Wnt3a transcripts are detected before *Fgf8* transcripts in the limb field ectoderm but not in the flank outside the limb fields. Subsequently, *Wnt3a* expression is up-regulated in the ectoderm cells near the dorsoventral (DV) border. *Fgf8* expression is initiated and then up-regulated within the region of high *Wnt3a* expression during AER formation. From stage 20 on, *Wnt3a* and *Fgf8* expression are confined primarily to the mature AER. Thus, *Wnt3a* expression appears to presage *Fgf8* expression and AER formation.

To verify the epistatic relationship between *Wnt3a* and *Fgf8* that is suggested by the expression data, we ectopically delivered each factor to developing limb buds. We misexpressed *Wnt3a* in the limb ectoderm using a replication-competent retroviral vector and assayed for the expression patterns of the various AER markers (*6*). Misexpression of *Wnt3a* induced ectopic expression of AER-specific genes, including *Bmp2*, *Fgf4*, and *Fgf8*, in broad patchy domains in the ectoderm of nearly 100% of infected limbs (Fig. 1E) (*5*). However, *Wnt3a* expression was not induced in the ectoderm by either fibroblast growth factor 4 (FGF4) protein or *Fgf8*-virus (*5*). This suggests that *Wnt3a* acts upstream of FGFs in establishing AER gene expression.

In addition to its effect on AER gene expression, *Wnt3a* misexpression occasionally led to disruption of the AER or to formation of an ectopic AER extending ventrally, or both (Fig. 1, E and F). These morphological effects on the AER are reminiscent of those seen after misexpression of *Radical fringe* (*7*). We therefore examined *Radical fringe* expression and found that it was ectopically expressed in *Wnt3a*-infected limbs (*8*). Disruption of the AER morphology was only seen in a subset of *Wnt3a*-infected limb buds, which is consistent with the finding that *Radical fringe* only affects AER formation when it is misexpressed at the earliest stages of limb development (*7*).

The FGFs produced in the AER are responsible for maintaining the proliferative state of the undifferentiated mesoderm at the distal tip of the limb bud, the progress zone (PZ) (*1*). To verify that the FGFs induced in the limb bud ectoderm by *Wnt3a* are functional signals, we examined the expression of several PZ markers: *Fgf10* (*9*), *Msx1* (*10*), *Nmyc* (*11*), and *Slug* (*12*). Equivalent results were obtained with each of these markers (Fig. 2) (*8*). When the AERs were removed from experimental limb buds, expression of the PZ markers was rapidly lost (Fig. 2, C and D). Application of *Wnt3a*-expressing cells to the AER-deprived limbs induced *Fgf8* expression and restored expression of the PZ markers (Fig. 2, E and F). To show that this response was due to the ectopic expression of FGFs and not to a direct action of *Wnt3a* itself, we removed the adjacent distal ectoderm as well as the AER so that the *Wnt3a* cells could not induce ectodermal *Fgf8* expression (Fig. 2G). Under these conditions, *Wnt3a* induced little or no expression of the PZ genes (Fig. 2H). The maintenance of the PZ is critical for outgrowth of the limb bud. The long-term effects of virally mediated *Wnt3a* misexpression, and consequent ectopic FGF production by the ectoderm, included some cases in which extra outgrowth formed digitlike structures (*5*). *Wnt3a* thus appears to influence both morphological AER formation and induction of AER-specific genes in the early limb bud.

The members of the vertebrate *Wnt* gene family have been categorized by their relative ability to transform murine mammary epithelial cells (*13*). A similar classification can be made on the basis of the ability to

M. Kengaku and C. J. Tabin, Department of Genetics, Harvard Medical School, 200 Longwood Avenue, Boston, MA 02115, USA.
J. Capdevila, C. Rodriguez-Esteban, J. De La Peña, J. C. I. Belmonte, The Salk Institute for Biological Studies, 10010 North Torrey Pines Road, La Jolla, CA 92037, USA.
R. L. Johnson, Department of Biochemistry and Molecular Biology, M.D. Anderson Cancer Center, University of Texas, 1515 Holcombe Boulevard, Houston, TX 77030, USA.

*These authors contributed equally to this work.
†Present address: Department of Biophysics, Kyoto University, Sakyo-ku, Kyoto 606, Japan.
‡To whom correspondence should be addressed. E-mail: belmonte@salk.edu
§The laboratories of these authors contributed equally to this study.

Molecular Basis for Interactions of G Protein βγ Subunits with Effectors

Carolyn E. Ford, Nikolai P. Skiba, Hyunsu Bae, Yehia Daaka, Eitan Reuveny, Lee R. Shekter, Ramon Rosal, Gezhi Weng, Chii-Shen Yang, Ravi Iyengar, Richard J. Miller, Lily Y. Jan, Robert J. Lefkowitz and Heidi E. Hamm

Science **280** (5367), 1271-1274.
DOI: 10.1126/science.280.5367.1271